OPERATIONAL APPROACH FOR THE MODELING
OF THE COMA DRAG FORCE ON ROSETTA

Carlos Bielsa[1]**, Michael Müller**[2] **and Ulrich Herfort** [3]

[1][2][3]*ESA/ESOC Flight Dynamics, HSO-GFS*
Robert-Bosch-Str. 5, 64293 Darmstadt, Germany
+49-6151-90-4253, Carlos.Bielsa@esa.int, Michael.Mueller@esa.int, Ulrich.Herfort@esa.int
[1]*GMV*
Isaac Newton 11, P.T.M., 28760 Tres Cantos (Madrid), Spain
+34-91-8072100, cbielsa@gmv.com

Abstract: *When Rosetta operates in the vicinity of its target comet, coma drag force will be comparable to the nucleus gravity force, while coma drag torque will be the dominant external torque. Hence, drag force and torque need to be estimated in order to predict spacecraft trajectory and angular momentum. This document outlines the operational approach devised at ESOC Flight Dynamics to account for the effect of the coma drag on the spacecraft dynamics. Several physical observables that provide information about the coma have been identified. For each of them, methods to reduce raw measurements to coma parameters have been developed. Processed data are stored in a database as function of position and time, and used to generate a coma drag acceleration file that is input for orbit determination. Moreover, an operational coma model, and a drag force and torque model have been put into place. They are used for orbit prediction and spacecraft angular momentum management. Reduction methods and models are based on physical assumptions, which need to be validated from measurements before being relied upon. Similarly, onboard instruments and payloads used to measure coma observables need to be calibrated before being used in operations. Finally, parameters of the models need to be updated to keep predictions consistent with observations. This document presents the selected observables, the reduction methods, the operational models, and the operational plan for validation of hypothesis, calibration of payloads and adjustment of models.*

Keywords: *Rosetta, coma, comet, drag, operations*

1. Introduction

The ESA mission Rosetta to 67P/Churyumov-Gerasimenko was designed to complete the most detailed study of a comet ever attempted. When the Rosetta spacecraft (SC) operates in the vicinity of its target comet at low heliocentric distance, the drag force exerted by the coma gas molecules is expected to be in the same order of magnitude as the gravity force from the comet nucleus. In addition, coma drag torque will be by far the dominant external torque on the SC. Hence, drag force and torque need to be estimated in order to predict the SC trajectory and angular momentum. This document outlines the operational approach devised at ESOC Flight Dynamics to account for the effect of the coma drag on the SC dynamics, a challenge never faced before.

Note that the severity of the effects of the coma on the SC will increase progressively over time, not only because the SC gets closer and closer to the comet, but also because the comet gets closer and closer to the Sun, with the resultant increase in comet outgassing. This progressivity shall facilitate the learning process, as well as the tuning of models and methods.
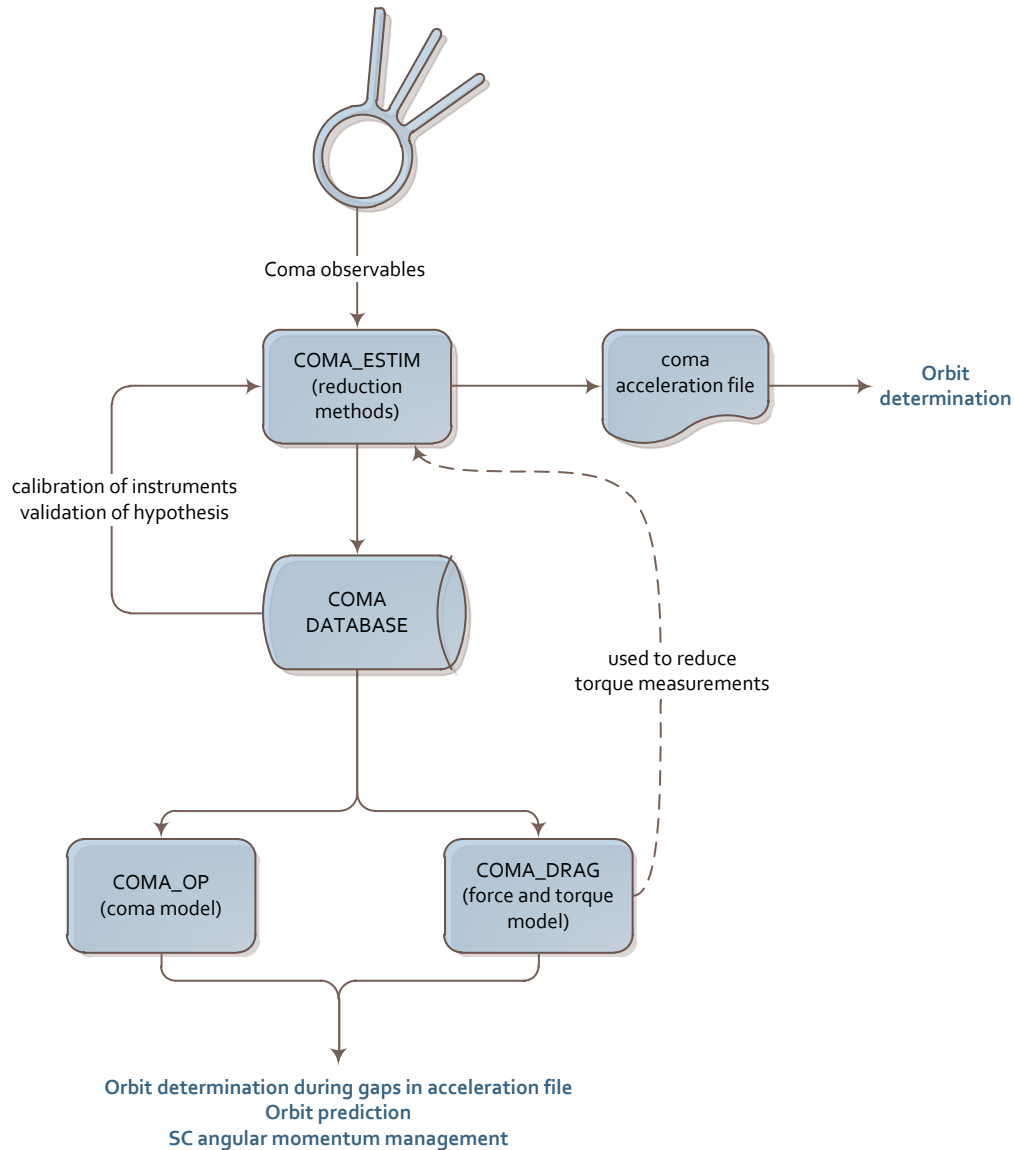
Figure 1 is an overview of the operational approach. Several physical observables that provide information about the coma state either at the SC position (in-situ observables) or at a distance (remote observables) have been identified. For each observable, methods to reduce raw measurements to a manageable number of variables specific to the observable have been devised. These processed data are stored in a database. Predictions of dynamic pressure from in-situ observables are used on a regular basis to generate an operational coma drag acceleration file that is used for orbit determination.

With this purpose, COMA_DRAG, a model that calculates the coma drag force and torque exerted on the SC for a given coma state and SC configuration has been implemented. Furthermore, COMA_OP, an operational coma model, has been put into place to predict coma gas state at different positions and times. While the coma drag acceleration file provides estimates of the effect of the coma on the SC for past flown trajectories and SC configurations, this operational coma model is used together with the coma drag model to predict the effect of the coma on the SC for potential trajectories yet to be flown. The model is also used for orbit reconstruction whenever in-situ measurements are either unavailable or uninformative (due to e.g. high attitude rate), as well as to predict the effect of the coma drag on reaction wheel levels for potential attitude profiles and wheel-offloading schedules.

Onboard instruments and payloads used to measure observables need to be calibrated before they can be used to derive information of the coma state. Moreover, reduction methods are based on physical assumptions, and these assumptions need to be verified before predictions can be relied upon. Similarly, parameters of the operational models need to be adjusted to actual observations if they are to provide reliable predictions.

Section 2 introduces the Rosetta SC with the relevant instruments and payloads. Section 3 present some basics of coma dynamics that are later used by the operational models and reduction methods. Section 4 looks at the design of the operational models COMA_OP and COMA_DRAG. Section 5 presents the coma observables and reduction methods. Finally, section

6 examines the initial setup of model parameters, as well as the operational plan for validation of hypothesis, calibration of instruments and payloads, and adjustment of model parameters from observations.


Figure 1. Overview of the operational approach for the modeling of coma drag force and torque on Rosetta

2. The Rosetta spacecraft

Rosetta is a spacecraft composed of a main body (the orbiter) and the Philae lander. The orbiter, stabilized on three-axes, consists of a central body with roughly cubic shape, an articulated High Gain Antenna (HGA) on the $+x_{sc}$ face and the solar arrays (SAs) on the $\pm y_{sc}$ faces. The lander is attached to the $-x_{sc}$ face. The solar arrays can be rotated around the y_{sc} axis and are always

sun pointing. Attitude control in normal mode is performed by means of four reaction wheels, while a system of eight thrusters is used during wheel off-loadings. Other onboard instruments relevant to this study are the two navigation cameras (NAVCAMs), nominal and redundant, with boresight along $+z_{sc}$. The NAVCAMs have a 1024x1024 pixel CCD and a field of view of 5 degrees. During the cometary phase, the $+z_{sc}$ side will typically be facing the nucleus, with y_{sc} perpendicular to the Sun.
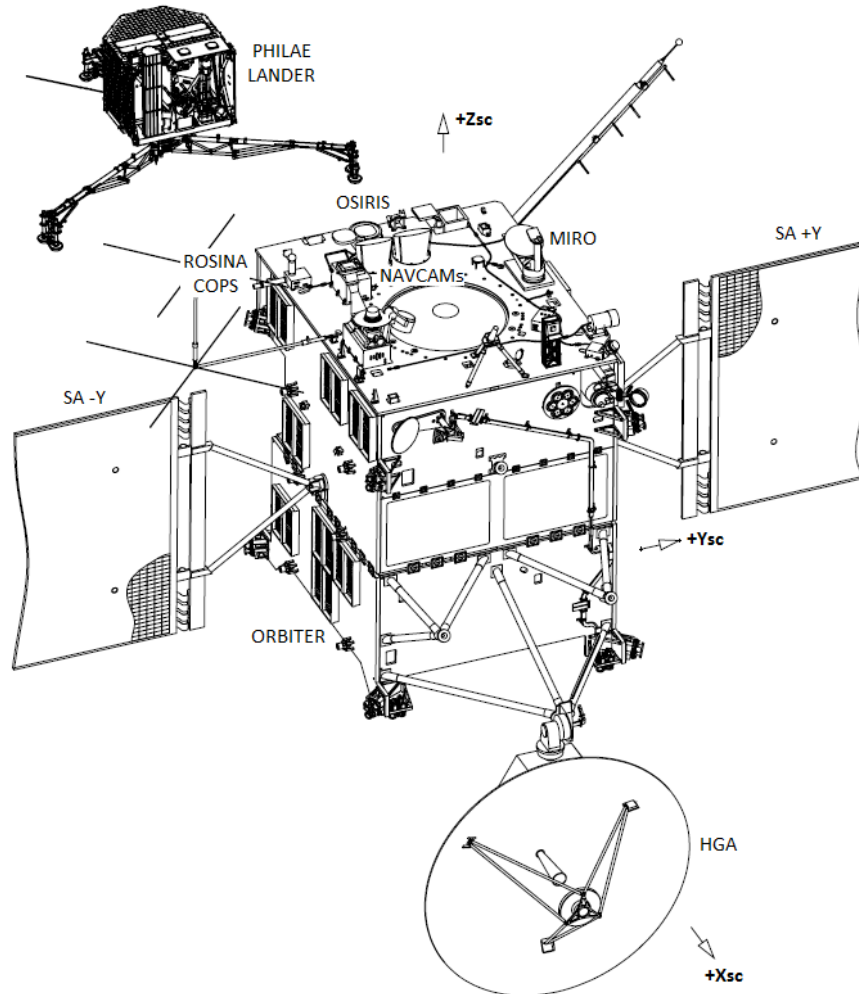
Figure 2. Rosetta spacecraft and SC axes. Modified from [3] with permission.

In addition to measurements from onboard instruments, inputs from three onboard payloads will be used for SC operations: OSIRIS, ROSINA COPS and MIRO, the three of them located on the $+z_{sc}$ side of the central body. OSIRIS, the Optical Spectroscopic and Infrared Remote Imaging System, is a science camera system with a 2048x2048 pixel CCD chip and two groups of lenses: the narrow-angle camera (NAC), with a field of view of 2.20x2.22 degrees, and the wide-angle camera (WAC), with a field of view of 11.35x12.11 degrees [1]. ROSINA, the Rosetta Orbiter Spectrometer for Ion and Neutral Analysis, incorporates the Comet Pressure Sensor (COPS), with a nude gauge mounted at the end of a boom and a ram gauge in an equilibrium chamber

opened towards $+z_{sc}$, capable of measuring in-situ total and ram pressures respectively. Finally MIRO, the Microwave Instrument for the Rosetta Orbiter, is a microwave detector with sub-millimeter channels specifically tuned to detect water remotely [2].

3. The coma

The target of Rosetta is 67P/Churyumov-Gerasimenko, a comet a few kilometers wide whose coma is believed to be mainly composed of H_2O, CO and CO_2 gas molecules, and a similar mass of dust particles. The bulk of dust mass is expected to be concentrated on large particles, than only reach small velocities relative to the nucleus [4]. Therefore, the dynamic pressure on the SC, responsible of drag force and torque, is expected to be dominated by interaction with gas molecules.

In the range where Rosetta operates, the gas state is well described by homogeneous Euler equations, i.e. external forces, heating and particle dissociations can be neglected. Moreover, the gas can be assumed to only interact along the radial direction relative to some fixed reference point in the nucleus. This way, the gas sublimated from the nucleus surface accelerates in radial adiabatic expansion, converging towards a relative velocity, common above all point on the nucleus surface, known as the terminal velocity. This convergence process is very quick, with the gas reaching the terminal velocity after having only traveled a few nucleus radii [4]. On what follows, we define function $\lambda(r)$ as the ratio of local gas velocity $v(r)$ to gas terminal velocity v_∞, with r being the distance from a given reference point in the nucleus (typically the nucleus center of mass), i.e.

$$\lambda(r) = \frac{v(r)}{v_\infty} \tag{1}$$

Furthermore, if r_1 and r_2 are the distances [m] to the gas source on the nucleus surface of two points along the same trajectory line, the equation of mass conservation along the radial direction can be written as [4]

$$\rho(r_1) \ v(r_1) \ r_1^{\ 2} = \rho(r_2) \ v(r_2) \ r_2^{\ 2} \tag{2}$$

with ρ denoting gas density [Kg/m^3] and v, gas velocity relative to the nucleus [m/s]. Note that for distances to the nucleus much larger than the nucleus width, r_1 and r_2 can also be thought of as distances to certain reference point in the nucleus (e.g. the nucleus center of mass).

Next, gas dynamic pressure is defined as

$$p_{dyn} = \frac{1}{2}\rho\, v^2 \tag{3}$$

From Eq. 1, 2 and 3 above, the ratio between the dynamic pressure at two radial distances r_1 and r_2 is given by

$$\frac{p_{dyn}(r_1)}{p_{dyn}(r_2)} = \left(\frac{r_2}{r_1}\right)^2 \frac{\lambda(r_1)}{\lambda(r_2)} \tag{4}$$

The interaction between the coma gas molecules and the SC surfaces is modeled assuming that a fraction α of gas molecules performs perfectly inelastic collisions while the remaining fraction $1-\alpha$ performs perfectly elastic collisions. Under this assumption, the drag force on a differential area dA with normal $\vec{n}$ exerted by coma gas with density ρ and relative velocity $\vec{v}$ to the differential area, is given by

$$d\vec{F} = \rho\, |\vec{v}\cdot\vec{n}|\, \left[\alpha\, \vec{v} + 2(1-\alpha)\, |\vec{v}\cdot\vec{n}|\, \vec{n}\right]dA \tag{5}$$

Fraction α is known as the accommodation coefficient and is in generally different for each SC surface. Because the velocity of the gas relative to the nucleus is expected to be an order of magnitude higher than the velocity of the SC relative to the nucleus, on what follows we employ the term "relative velocity" and the symbol $\vec{v}$ for both gas velocity relative to the SC and to the nucleus. Next, let $\vec{e}_{flw}$ denote the direction of vector $\vec{v}$ and v denote its norm, i.e. $\vec{v} = v\, \vec{e}_{flw}$. If Φ denotes the angle between $\vec{e}_{flw}$ and $\vec{n}$, Eq. 5 can be written as

$$d\vec{F} = 2\alpha\, p_{dyn} |\cos\Phi| dA\, \vec{e}_{flw} + 4(1-\alpha)p_{dyn}\cos^2\Phi\, dA\, \vec{n} \tag{6}$$

From Eq. 6, it is apparent that whatever the accommodation coefficient, drag force is proportional to dynamic pressure.

While the dynamic pressure supported by the SC is mostly due to interactions with gas molecules, optical images of the coma are expected to be dominated by light scattered by dust particles. The $Af\rho$-parameter [m] is often used as a proxy of dust production rate, as under certain conditions it is largely independent of observational circumstances. It is obtained by calculating the total intensity detected on the pixels inside the field of view of an observation centered at the comet center, and scaling it with some observational parameters. In particular, if the coma is in steady state, there is no particle fragmentation and the particles move on straight trajectories relative to the nucleus, then the $Af\rho$-parameter of observations centered at the comet center is independent of heliocentric distance, distance from the observer to the comet, and field

of view. Moreover, if dust albedo is independent of the wavelength, then the $Af\rho$-value is also independent of the filter used during the observation.

4. The models

4.1. The operational coma model: COMA_OP

An operational coma model, COMA_OP, has been implemented at ESOC Flight Dynamics to predict coma gas dynamic pressure and gradient at each position and time. The estimated coma state is used operationally both for orbit determination when direct predictions of drag acceleration are either unavailable or uninformative (due to e.g. high SC attitude rates), and for orbit propagation into the future. COMA_OP is also used for SC angular momentum management, to ensure that reaction wheel levels will remain within operational limits for a given commanded attitude profile and wheel off-loadings schedule.

The coma state is modelled by superposition of the states of a finite number of gas species, each originating at a certain source. COMA_OP uses two coma reference frames to define the dynamics of the coma, one with one axis aligned with the comet-Sun direction, and the other attached to the nucleus and corotating with it. The position of each gas source origin can be defined in either coma reference frame. This way, if the coma turns out to have on top of the Sun-driven background activity a strong stable gas jet clearly localized at certain point on the nucleus surface, it would be possible for COMA_OP to represent the morphology of the coma by combining a source relative to the Sun to model the background activity with a source attached to the nucleus to model the localized gas jet.

For each source, fields of gas density and velocity vector relative to the nucleus are defined by a set of input parameters than can be tuned to adjust the model to measurements of coma observables. At each position, gas velocity vector is radial with respect to the source origin and with norm equal to $\lambda(r)\ v_\infty$, where r is the distance to the source origin and v_∞ is the gas terminal velocity, an input parameter of the model. Function $\lambda(r)$ is initially set to 1 (i.e. source gas velocity is the same everywhere) but different functions $\lambda(r)$ can be incorporated into the model if the calibration of gas velocity versus distance described in section 6.3 advises to do so. For the modeling of the gas density field, a source boundary sphere of radius r_0 is defined with center at each source origin. Spherical coordinates { r, θ, φ } are defined for each of the sources, and gas density at each position on the source boundary sphere $r = r_0$ is given via a spherical harmonics distribution of a certain order l_{max} :

$$\rho_0(\theta,\varphi,t) = a_0^0(t) + \sum_{l=1}^{l\,max}\left[a_l^0(t)P_l^0(\cos\theta) + \sum_{m=1}^{l} P_l^m(\cos\theta)\big(a_l^m(t)\cos m\varphi + b_l^m(t)\sin m\varphi\big)\right] \qquad (7)$$

7

In the expression above, θ and φ are declination and right ascension in the source spherical coordinates, $a_0^0(t)$, $a_l^0(t)$, $a_l^m(t)$ and $b_l^m(t)$ are the spherical harmonic coefficients, and P_l^m are the associated Legendre polynomials. The spherical harmonic coefficients can in turn be expressed as periodical functions of time via a Fourier series of a certain order. It is the coefficients of the Fourier series of each spherical harmonic coefficient that are, for each of the sources, input to the model.

Another element taken into account in COMA_OP is the heliocentric distance. For some gas species, the mass flow leaving the nucleus surface is related to the surface temperature, so that the closer the Sun is to the comet, the higher the species density. This effect is modelled with a factor $(d_k / r_h(t))^{\alpha_k}$, where $r_h(t)$ is the heliocentric distance at time t, and d_k and α_k are input parameters of the model, piecewise defined for each interval k of heliocentric distances. (Note that there is a twofold dependency of COMA_OP on time: first, density is allowed to periodically change with time through Fourier series; second, density may increase monotonically with time as the comet approaches perihelion).

Finally, from the mass conservation law given by Eq. 2, the evolution of gas density with source distance is incorporated via a factor $(r_0 / r)^2 \; \lambda(r_0)/\lambda(r)$.

All in all, the density of a gas species at position { r,θ,φ } and time t is given by

$$\rho(\theta,\varphi,r,t) = \left(\frac{r_0}{r}\right)^2 \frac{\lambda(r_0)}{\lambda(r)} \left(\frac{d_k}{r_h(t)}\right)^{\alpha_k} \rho_0(\theta,\varphi,t) \qquad (8)$$

Further analytical expressions have been derived that provide gradients of velocity and density at each position and time. From these outputs, it is straightforward to calculate the dynamic pressure and gradient of dynamic pressure for each of the sources. Finally, the overall coma dynamic pressure and gradient are calculated by adding up the contributions from each individual source. Note that coma state and gradients returned by COMA_OP are continuous in both position and time.

Indeed, the analytical approach to the modeling of the coma implemented in COMA_OP and outlined above fulfils the operational requirements of moderate execution time and continuity of outputs, while representing the morphology of a typical coma with a set of parameters easily adjustable to empirical observations.

4.2. The drag force and torque model: COMA_DRAG

A drag force and torque model known as COMA_DRAG has been implemented at ESOC Flight Dynamics to predict the force and torque exerted by the coma gas drag on the Rosetta SC.

The inputs to COMA_DRAG are incoming flow direction $\vec{e}_{flw}$, dynamic pressure, gradient of dynamic pressure and SC configuration, the latter defined by the articulation angles of both HGA and SAs and a flag indicating whether the lander is present. From these inputs, COMA_DRAG calculates drag force and torque on the SC considering both shadowing between SC units and specific accommodation coefficients for each unit surface.

In order to reduce computational time in the calculation of shadowings, an analytical approach has been favored over the traditional computationally-intensive iterative method that considers intersections inside grid cells of decreasing size until a target accuracy is achieved. In fact, to increase simplicity, the model has been designed *ad hoc* for the specific geometrical characteristics of the Rosetta SC (e.g. in Rosetta the HGA and the lander cannot shadow each other because the central body is in between for every possible configuration, hence shadowings between HGA and central body need not to be computed).

For the purposes of COMA_DRAG, the Rosetta SC is split into five units, each model as a polyhedron: the central body, modeled as a rectangular cuboid; the lander; the two SAs, each modeled as a rectangle with two sides; and the HGA. For the HGA, two different polyhedra are considered depending on whether the incoming gas flow is rather aligned with the antenna boresight or perpendicular to it. The modeling of the HGA edge-on area is important because the resulting drag torque can be significant, hence the HGA cannot be modeled as a flat disk.

The calculation process of COMA_DRAG is as follows. First, for the input SC configuration given by SAs and HGA articulation angles, and the lander presence, a polygon in SC frame is constructed for each unit surface that is facing the flow. Second, a bunch of properties are defined for each of these polygons, including area, normal vector, accommodation coefficient and flags that indicate the actual SC unit surfaces the polygons are associated with. Third, a projection plane perpendicular to the incoming flow and containing the SC center of mass is constructed. All polygon vertices are then projected along the flow direction $\vec{e}_{flw}$ onto the projection plane.

Fourth, a two-step sequence of intersections on the projection plane is performed. In the first step, intersections involve one face of the central body and one face of one of the appendages (HGA or lander). Each time an overlap between two projected polygons is detected, the intersection is analytically computed. This 2-dimensional intersection polygon on the projection plane is then propagated backwards to the 3-dimensional space to one of the SC surfaces to which the intersection polygon belongs, in particular to the SC surface that is at least partially hidden by the other SC surface. This intersection polygon is then added to the initial list of polygons, inheriting the accommodation coefficient from the parent polygon that is at least partially hidden and with flags indicating that is the result of a single-intersection of polygons. Once the first step is complete, a second step is initiated with intersections between the SAs and the polygons from the first step, including both polygons associated with actual central body and appendage unit faces, and the new polygons that were created from the intersections of the first step. In the latter case, a double-intersection polygon (i.e. an overlap between three polygons) might be created, again projected backwards to the most hidden polygon and inheriting its accommodation coefficient, and with flags indicating that is associated with a double-intersection.

At last, overall drag force and torque is calculated by adding (for unit polygons and double-intersection polygons) and subtracting (for single-intersection polygons) the contributions to force and torque from the different polygons. This is done by splitting every polygon into triangles and calculating force and torque on each triangle from analytical integration over the triangle of the force and torque exerted on each differential area by the linear field of dynamic pressure. Drag force on a differential area is calculated with Eq. 6.

Figure 3. shows the intersections of projected polygons on the projection plane, as calculated by COMA_DRAG. In this particular example, the sequence of intersections results in 17 polygons: 3 for the central body sides facing the flow, 2 for the SAs, 1 for the HGA, 3 for the lander sides facing the flow, 7 for single intersections between unit surfaces, and 1 for the double intersection that results from a lander face being in front of a central body face that in turn is in front of a SA face.
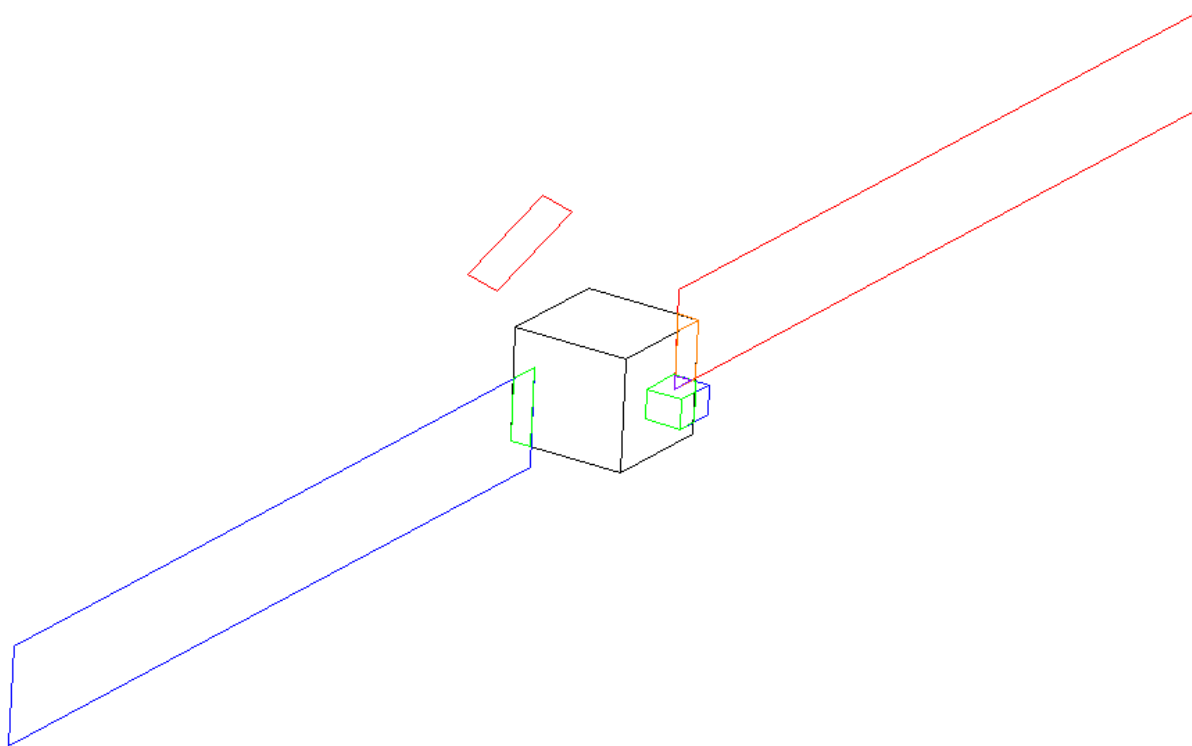
Figure 3. Intersections of projected polygons on projection plane as calculated by COMA_DRAG

5. Coma observables and reduction methods

A number of physical observables that provide information about the coma state either at the SC position (in-situ observables) or at a distance (remote observables) have been identified. Four

among them have been selected to gather information about the coma that can later be used to predict drag force and torque on the SC, and hence inform SC planning and operations.

Selected in-situ observables are torque measurements and ROSINA COPS measurements. Torque measurements are derived from the reaction wheels levels in telemetry plus the commanded attitude profile. ROSINA COPS total pressure readings from the nude gauge can be transformed into gas density values. Similarly, ram pressure readings from the COPS ram gauge can be transformed into values of radial gas flow (i.e. density times radial velocity). Because radiometric data are also affected by gravity, they are not foreseen to be used to estimate coma state. Moreover, onboard accelerometers are not expected to be sufficiently sensitive to detect drag acceleration except during close fly-bys around perihelion.

Regarding remote observables, selection includes images of the coma in the visual wavelength from the NAVCAMs and OSIRIS WAC, and measurements from MIRO. Images of the coma are dominated by light scattered by dust particles, but information about the gas distribution could be extracted from the dust distribution.

Moreover, calibrated spectra from MIRO measurements can be reduced to water density at the closest approach point (CA) of a given line of sight (LOS) and possibly to other water parameters. At perihelion, water molecules in the coma will dominate the drag force. Therefore, remote detection of water molecules by MIRO will be required if either the SC trajectory is to enter regions never flown before, or the coma structure changes significantly with time.

5.1. Torque measurements

Reaction wheel data are processed in two steps.

In the first step, the external torque on the SC is derived from measured reaction wheel levels and the commanded SC attitude profile and associated attitude rate. With this purpose, the SC angular momentum in inertial frame $\vec{L}_{in}$ is calculated for all RW telemetry records within processing time intervals of certain duration (e.g. 5 minutes) with the expression

$$\vec{L}_{in} = A^T (I\vec{\omega} + \sum_j h_j \vec{e}_{RWj}) \tag{9}$$

where A is the commanded attitude matrix (that converts a vector expressed in inertial frame $\vec{r}_{in}$ to SC frame $\vec{r}_{sc}$ by $\vec{r}_{sc} = A\vec{r}_{in}$), $\vec{\omega}$ is the attitude rate associated to the commanded attitude profile and expressed in SC frame, I is the inertial tensor of the SC relative to its center of mass (COM) and expressed in SC frame, and h_j is the angular momentum of wheel j around its axis $\vec{e}_{RWj}$, with $j = 1,4$.

Next, estimates of $\vec{L}_{in}$ within each processing interval are fitted by linear regression to a straight line, which leads to an estimated external torque in inertial frame $d\vec{L}_{in}/dt$.

Estimates of $\vec{L}_{in}$ are only reliable within time intervals with smooth SC dynamics. For this reason, only time intervals that fulfill certain criteria are used in subsequent processing. Filtering criteria include low attitude rates, low SA and HGA articulation angular speeds, enough tranquilization time since last use of thrusters (during wheel off-loadings or orbit control maneuvers), and residua of the measured points relative to the fitted line lower than a threshold.

For each time interval that fulfills these criteria, the estimated torque in SC frame at the interval mid-time t is calculated by $\vec{T}_{sc} = A\,d\vec{L}_{in}\big/dt$.

In a second step, the dynamic pressure is estimated from the measured torque $\vec{T}_{sc}$ at each time t.

The torque due to drag is estimated by subtracting from the overall estimated torque $\vec{T}_{sc}$ the estimated solar radiation pressure torque $\vec{T}_{srp}$, i.e. $\vec{T}_{drag} = \vec{T}_{sc} - \vec{T}_{srp}$. Next, the coma force and torque model COMA_DRAG described in section 4.2 is called at each time t with input dynamic pressure of 1 N/m^2, null dynamic pressure gradient, estimated gas flow direction $\vec{e}_{flw}$, and actual SC configuration (this includes SA and HGA articulation angles and lander presence flag). Let us refer to this predicted drag torque per unit of dynamic pressure as $\vec{T}_1$, i.e. $\vec{T}_1 =$ COMA_DRAG(1 N/m^2, {0,0,0} N/m^2/m, $\vec{e}_{flw}$, SC configuration).

If the norm of $\vec{T}_1$ is far from zero, the dynamic pressure is estimated by

$$p_{dyn} = 1\frac{N}{m^2}\frac{\vec{T}_1}{\left\|\vec{T}_1\right\|^2}\cdot\vec{T}_{drag} \tag{10}$$

Note that the equation above equates the components along the model drag torque $\vec{T}_1$ of the measured drag torque $\vec{T}_{drag}$ and the model drag torque $p_{dyn}\vec{T}_1$.

The quality of the estimation of dynamic pressure with the method described above is tied to the validity of the assumptions of negligible torque due to dynamic pressure gradients, actual gas flow direction close to $\vec{e}_{flw}$ and negligible change in flow direction in the time interval during which $\vec{T}_{sc}$ was measured. Hence, certain criteria must be fulfilled for estimates of p_{dyn} to be considered informative. Filtering criteria include small variation of estimated dynamic pressure under variation of flow direction, norm of $\vec{T}_1$ far from zero, small angle between the measured drag torque $\vec{T}_{drag}$ and model drag torque $\vec{T}_1$, and direction of $\vec{T}_{drag}$ far from direction $\pm\,\vec{y}_{sc}\times\vec{e}_{flw}$ (to ensure that torque is not dominated by coma gradients).

For all estimates of dynamic pressure that fulfill the filtering criteria, the dynamic pressure vector is estimated as $p_{dyn}\vec{e}_{flw}$.

5.2. ROSINA COPS pressure readings

The ROSINA COPS sensor has a nude and a ram gauges that provide pressure readings p_g [mbar], with index g identifying the gauge, i.e. g is either "nude" or "ram". Each gauge can be run in different configurations, abbreviated by the letter c, which for the nude gauge depend on the active filament, and its ion and emission range, while for the ram gauge depend on the enabled microtips, as well as their ion and emission range.

ROSINA/COPS pressure readings are processed in two steps. The reduction process described below is run independently for the two gauges.

In the first step, COPS pressure readings are averaged within intervals of a certain duration (e.g. 5 minutes). Only intervals of time sufficiently separated from the last thruster actuation and during which the COPS configuration c of the respective gauge remains constant are considered for further processing. For these time intervals, mean value $\bar{p}_g$ and standard deviation σ are evaluated.

In a second step, averaged measured pressures are converted to in-situ dynamic pressures. For the nude gauge, the following expression is used

$$p_{dyn} = C_{nude,c}\bar{p}_{nude}\lambda(r)^2 \tag{11}$$

where $C_{nude,c}$ is the calibration factor for configuration c of the nude gauge and $\lambda(r)$ is the ratio of gas velocity to gas terminal velocity, as defined in section 3. Meanwhile, for the ram gauge, the expression below is used

$$p_{dyn} = \frac{C_{ram,c}\bar{p}_{ram}}{-\vec{e}_{flw}\cdot\vec{z}_{sc}}\lambda(r) \tag{12}$$

with $C_{ram,c}$ being the calibration factor for configuration c of the ram gauge. The rationale of Eq. 11 and 12 above is that nude gauge pressure readings are proportional to gas density ρ, ram gauge pressure readings are proportional to gas flow $\rho\vec{v}$ along $-\vec{z}_{sc}$, and the dynamic pressure is defined as $p_{dyn} = 1/2\rho v^2$.

For dynamic pressure estimates to be considered valid, it is required both that the calibration factor $C_{g,c}$ used for that gauge and configuration is available (see section 6.4 for calibration of ROSINA COPS) and that the angle between $-\vec{z}_{sc}$ and the direction of the incoming flow $\vec{e}_{flw}$ is below a threshold.

For all estimates of dynamic pressure that fulfill the filtering criteria, the dynamic pressure vector is estimated as $p_{dyn}\vec{e}_{flw}$.

5.3. MIRO spectra

The MIRO team coverts MIRO raw data into tables of measured antenna temperature versus frequency, known as calibrated spectra, from which different parameters of the coma can be derived. Although it is only foreseen to exchange data for water species, calibrated spectra might also be exchanged between the MIRO team and ESOC Flight Dynamics for other frequency bands.

With the purpose of reducing calibrated spectra to coma parameters relevant for SC operations, several retrieval methods have been envisaged, each relying on certain physical assumptions and providing different parameters of the coma. An assumption common to all methods is that water molecules close to the CA of the LOS are in thermal equilibrium. It is expected that this condition is always fulfilled if the comet is very active (e.g. near perihelion) and CA is not more than 100 km from the nucleus.

The first retrieval method, referred to as R00 and developed at ESOC Flight Dynamics, provides estimated temperature [K] and number density [#/m^3] of a water isotopologue at MIRO LOS CA. Inputs to the retrieval method are two spectra for two different water isotopologues that were taken simultaneously. The method requires that for one of the observed isotopologues the coma is optically thick (this is expected to be the case for $H_2^{16}O$) and for the other, optically thin (this is expected to be reasonably well fulfilled for $H_2^{17}O$).

In a second step, the number density n_i of the ortho H_2O isotopologue i at LOS CA is converted to dynamic pressure at that same position by the equation

$$p_{dyn} = D_i n_i \lambda (r_{CA})^2 \tag{13}$$

where D_i is a scaling factor and r_{CA} is the distance from the comet center to LOS CA. The dynamic pressure vector at LOS CA is then estimated as $p_{dyn}\vec{e}_{flw}$.

A second retrieval method, referred to as R01 and developed by the MIRO team, provides and estimate of the outgassing rate of ortho-water and the velocity profile. Inputs are spectra for two different water isotopologues, recorded close in time with various angles of the LOS with respect to the nucleus center, all LOS and the nucleus center lying on one plane. Underlying assumptions are that the coma is radial-symmetric and that water temperature as a function of cometocentric distance is known.

5.4. Camera images

Optical images of the coma will be regularly available from the NAVCAMs and OSIRIS WAC.

For each of the images, a cometocentric grid in polar coordinates is defined on the image plane. The width of cells is adjusted such that coma variations average out. The purpose of the reduction of camera images is to convert the intensity of the pixels on the image plane (a bi-

dimensional array) into some proxy of averaged dust activity as a function of azimuth (a one-dimensional array) that can be easily stored and processed when required. This indeed requires an accurate understanding of the radial evolution of the dust state. For each cell, magnitude $J / I_{sun}^{(filter)}$ and the $Af\rho$-value [m] are averaged over all pixels that fall in that cell, where J is the radiance received [W/m^2/sr], $I_{sun}^{(filter)}$ is the intensity of the Sun at the heliocentric distance of the comet seen through the filter of the camera in use [W/m^2/sr], and the $Af\rho$-value of each pixel is calculated with the expression

$$Af\rho = 8\pi^2 \frac{d_{CA}}{\Delta u} \frac{J}{I_{sun}^{(filter)}} \tag{14}$$

with d_{CA} being the CA distance of the LOS [m] and Δu, the angle covered by points along the LOS in front of the camera as seen from the comet center [rad].

The selection of an appropriate grid and the subsequent averaging process are carried out with help of a graphical user interface (GUI). Figures 4 and 5 are screenshots of the GUI implemented at ESOC Flight Dynamics showing grid selection and the averaged distribution of $Af\rho$-values. In Fig. 5, cell azimuth is displayed in the horizontal axis whereas each cell distance to comet center is showed in a different line. In this case, all lines are superimposed because an idealistic simulated image was used as input and so the $Af\rho$-parameter is completely independent of the radius in the field of view, but with real-world images the reduction to a one-dimensional array of azimuths may prove more challenging.
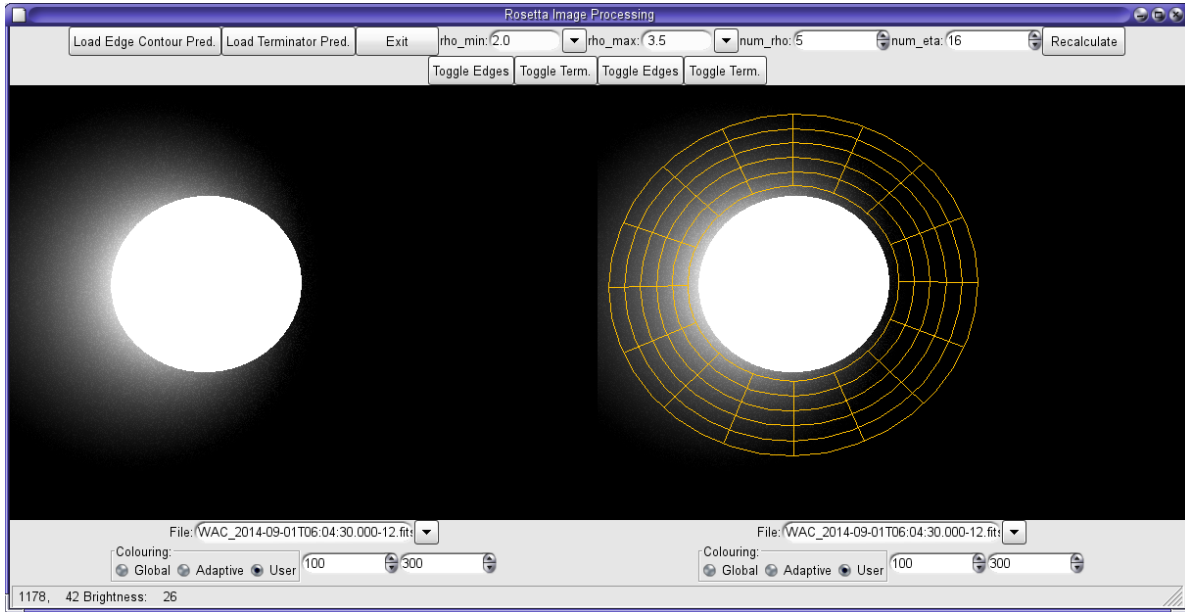
Figure 4. Screenshot of GUI with grid definition for a simulated idealistic WAC image of the coma dust. The nucleus is represented as a white circle.

15
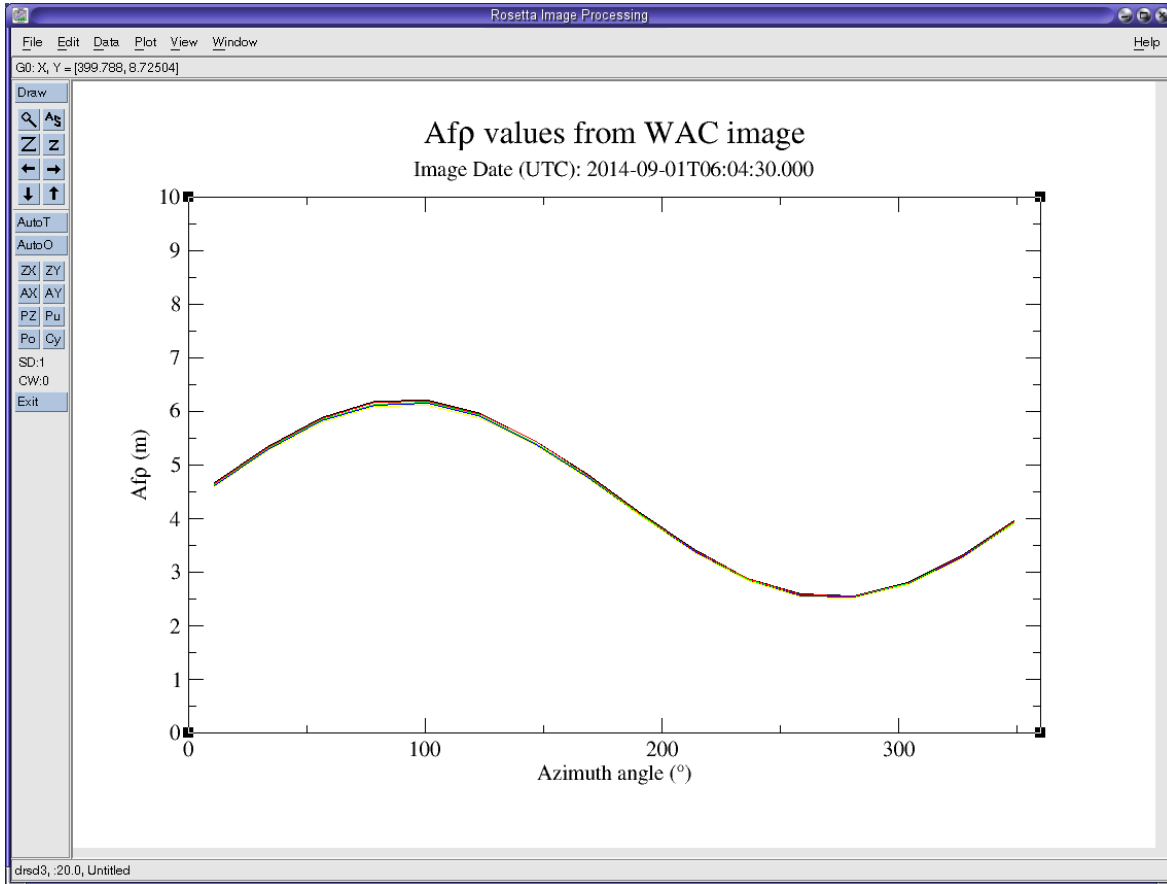
Figure 5. Screenshot of GUI with averaged *Afρ* values from a simulated idealistic WAC image.

6. Initial setup, validation and calibration

All payloads measuring observables need to be calibrated before they can be used to derive information about the coma that can in turn be used to inform spacecraft operations. Similarly, all assumptions underlying the observable reduction methods need to be validated before the reduction methods can be trusted. All such calibrations and validations will be performed internally in ESOC Flight Dynamics according to the schedule outlined in Tab. 1. First, it is verified that the effect of dynamic pressure gradients on the SC drag torque can be neglected. Only then the method to reduce torque measurements to gas dynamic pressure in section 5.1 can be relied upon. Meanwhile, the ratio of ram to nude pressure from ROSINA COPS is used to calibrate gas velocity function $\lambda(r)$. Next, ROSINA COPS gauges are individually calibrated from torque measurements and the function $\lambda(r)$. At this point, the validity of the R-squared scaling can be confirmed from ROSINA COPS measurements (and the $\lambda(r)$ function if the nude gauge is used). Next, MIRO is calibrated with in-situ measurements of torque and ROSINA.

16

Moreover, the coefficients of COMA_OP are periodically updated from ROSINA, torque and MIRO measurements at different positions and times. Finally, reductions of images from the NAVCAMs and OSIRIS WAC are contrasted against the gas state database to derive scaling laws to convert observed dust state into gas state .

Table 1. Schedule for calibration of observables and validation of assumptions from measurements

Stage		Observable or assumption							
		Torque measurements	$\lambda(r)$	ROSINA	R-squared scaling	MIRO	Spatial distribution	Temporal evolution	Optical images
Stage	**Before coma measurements**	Unreliable if significant density gradients	Assumed 1	Unreliable	Assumed valid	Unreliable	Assumed axialsymmetric	Based on Earth-based observations	Unreliable
	Monitoring of density gradients	Reliable (once gradients confirmed negligible)	Assumed 1	Unreliable	Assumed valid	Unreliable	Assumed axialsymmetric	Based on Earth-based observations	Unreliable
	Calibration of $\lambda(r)$ *	Reliable	Calibrated	Unreliable	Assumed valid	Unreliable	Assumed axialsymmetric	Based on Earth-based observations	Unreliable
	Calibration of ROSINA	Reliable	Calibrated	Calibrated	Assumed valid	Unreliable	Assumed axialsymmetric	Based on Earth-based observations	Unreliable
	Validation of R-squared scaling	Reliable	Calibrated	Calibrated Used as input	Validated	Unreliable	Assumed axialsymmetric	Based on Earth-based observations	Unreliable
	Calibration of MIRO	Reliable	Calibrated	Calibrated	Validated	Calibrated	Assumed axialsymmetric	Based on Earth-based observations	Unreliable
	Calibration of spatial distribution (COMA_OP)	Reliable	Calibrated	Calibrated	Validated	Calibrated	Calibrated	Based on Earth-based observations	Unreliable
	Calibration of temporal evolution (COMA_OP)	Reliable	Calibrated	Calibrated	Validated	Calibrated	Calibrated	Calibrated	Unreliable
	Conversion from dust to gas distribution	Reliable	Calibrated	Calibrated	Validated	Calibrated	Calibrated	Calibrated	Calibrated

* Calibration of $\lambda(r)$ is done with ROSINA ram to nude gauge pressure ratio $\overline{p}_{ram}/\overline{p}_{nude}$, for which the gauges need not be calibrated.

** Color code:
    - cells in light red indicate that the observable/assumption is unreliable after that stage
    - cells in light green and **dark green** indicate that the observable/assumption is calibrated/validated after that stage
    - cells in **dark green** indicate that the observable/assumption is used as input for that stage

6.1. Initial setup

In the initial setup, until measurements from Rosetta instruments and payloads yield contrary evidence, the distribution of gas density in the coma is assumed to be axial-symmetric, with maximum density over the subsolar point and a cosine dependency with the phase angle, i.e. $\rho \propto a\cos\theta + b$, with a and b being constants, and θ, the phase angle, defined as the angle with the Sun as seen from the comet center. Gas velocity is assumed to be radial with respect to

the nucleus COM. It is assumed that gas has reached its terminal velocity v_∞ in the range of cometocentric distances where Rosetta operates, with terminal velocity values derived from Earth-based observations that rank between 620 m/s at 3.5AU to 800 m/s at perihelion. Furthermore, it is considered that a single representative gas species with averaged properties suffices to represent the dynamic effects of the coma on the spacecraft. The coma gas production rate at each heliocentric distance is set equal to the maximum expected value from Earth-based observations, that varies from 17 Kg/s at 3.5 AU to 380 Kg/s at perihelion. Collisions between gas molecules and SC surfaces are assumed to be perfectly inelastic.

In terms of the parameters of the coma model COMA_OP, all the above implies that $\lambda(r) = 1$, there is a single source located at the nucleus COM with spherical coordinates defined relative to the Sun, and the spherical harmonics distribution that defines the density in spherical coordinates has order $l_{max} = 1$ with $a_1^1(t) = b_1^1(t) = 0$. The only non-zero spherical coefficients, a_0^0 and a_1^0, are independent of time. Note also that $\vec{e}_{flw}$ is always aligned with the position vector relative to the nucleus COM. Regarding the force and torque model COMA_DRAG, the accommodation coefficient of all SC surfaces is initially set to 1.

6.2. Monitoring of density gradient

For an axial-symmetric coma and at the cometocentric distances where Rosetta operates, the SC torque due to density gradients is expected to be negligible with respect to the SC torque due to SC asymmetries.

Nevertheless, if the coma turns out to be far from axial-symmetric, the contribution of density gradients to SC torque might be significant. In this scenario, accurate local predictions of coma state would be impossible, and the approach would be instead to provide integral predictions of the coma effect on the SC over arcs of a certain length.

For this reason, it is important to monitor coma density gradients. This will be done from in-situ estimates of coma drag torque from RW levels (see section 5.1). Because the contribution of overall torque due to SC asymmetries is dominated by the HGA, this torque is approximately align with $\pm y_{sc}$ (the HGA arm is on the plane xz_{sc} and the gas flow typically comes from $-z_{sc}$). Conversely, the torque due to coma gradients is mainly driven by the SAs, which are mounted along $\pm y_{sc}$, and hence the resulting torque is approximately aligned with $\pm x_{sc}$ if gas flow comes from $-z_{sc}$.

Therefore, the ratio between the $\pm x_{sc}$ and the $\pm y_{sc}$ components of the coma drag torque when $+z_{sc}$ points to comet nadir will be monitored as an indication of the importance of coma gradients, with large values associated to significant gradients.

If as expected, dynamic pressure gradients have a negligible effect on SC drag torque, then estimation of dynamic pressure from torque measurements as described in section 5.1 can be considered reliable.

6.3. Calibration of gas velocity versus distance

The ratio of ROSINA COPS ram and nude gauge pressures $\overline{p}_{ram}/\overline{p}_{nude}$ is proportional to the gas velocity when $\vec{z}_{sc}$ is pointing to the comet (see section 5.2).

If measurements of this ratio are available at different distances from the comet, they can be used to calibrate the function $\lambda(r)$, defined in section 3. Alternatively, measurements from MIRO can be used to calibrate function $\lambda(r)$ or validate the calibration done with ROSINA measurements (see retrieval method R01 in section 5.3).

An update of function $\lambda(r)$ is only foreseen if its value deviates significantly from 1.

6.4. Calibration of ROSINA COPS

Based on time intervals during which in-situ estimates of drag torque (reduced from RW levels in telemetry as described in section 5.1) and pressure readings from ROSINA COPS gauges are available for a given configuration c, the calibration factors $C_{g,c}$ and their standard errors are calculated as the arithmetic mean of $p_{dyn,trq}/\left(\overline{p}_g \lambda^2(r)\right)$ for ROSINA COPS nude gauge and $p_{dyn,trq}/\left(\overline{p}_g \lambda(r)/\left(-\vec{e}_{flw}\cdot\vec{z}_{sc}\right)\right)$ for ROSINA COPS ram gauge, where $p_{dyn,trq}$ is the dynamic pressure estimated from the reduction of RW levels in telemetry, as described in section 5.1.

The calibration factor is made available for processing of the COPS data of gauge g in the configuration c if the ratio of the standard error to the calibration factor is smaller than a threshold.

Note that if, as expected, gas terminal velocity increases as the comet approaches perihelion, COPS calibration factors will need to be recalculated to account for the increase in terminal velocity.

6.5. Validation of R-squared scaling versus distance

The operational coma model COMA_OP assumes that the flux from a given source [Kg/m^2/s] decreases according to an inverse square law along the flow direction (see section 4.1). This assumption can be validated by multiplying the ROSINA COPS ram pressure (taken while $\vec{z}_{sc}$ is pointing to the comet) with the square of the distance and comparing measurements taken at different distance but along the same flow direction and over the same point on the comet. The same validation can be performed with nude gauge pressures multiplied by $\lambda(r)$.

6.6. Calibration of MIRO

MIRO measurements of type R00 provide estimates of the density of an ortho water isotopologue at LOS CA (see section 5.3).

For determining an empirical calibration factor that allows converting the R00 measurement into a dynamic pressure it is required to have in-situ measurements available over the same point on the nucleus (from ROSINA or torque measurements).

MIRO operational observations are scheduled during navigation slots using OSIRIS WAC, with an SC attitude for which MIRO LOS passes only a few kilometers away from the nucleus. Because Rosetta operates at larger distances, it cannot be assumed that in-situ measurements at the same distance from the comet are available. Therefore a dynamic pressure p_{dyn} measured in situ at distance r from the nucleus center is scaled to the closest approach distance r_{CA} of the LOS with Eq. 4, resulting in

$$p_{dyn,CA} = \left(\frac{r}{r_{CA}}\right)^2 \frac{\lambda(r_{CA})}{\lambda(r)} p_{dyn} \tag{15}$$

The calibration factor D_i in Eq. 13 to convert an R00 measurement to dynamic pressure is then given by

$$D_i = \frac{p_{dyn,CA}}{n_i \lambda(r_{CA})^2} \tag{16}$$

Note that the validation of the R-squared scaling versus distance performed in section 6.5 is only performed for distances in which Rosetta operates, i.e. extrapolation of the scaling law is required.

6.7. Calibration of the spatial distribution

In this section we describe how measurements can be used to update either the gas production rate or the spatial distribution in COMA_OP.

The methods described in sections 5.1, 5.2 and 5.3 provide a list of estimates $\left(p_{dyn} \vec{e}_{flw}\right)_i$ from measurements at certain times and positions. A subset of these estimates is selected based on the underlying observable (torque, COPS or MIRO), and the time and cometocentric distance at which the measurements were made.

The selected estimates are then scaled to the reference distance r_0 defined in section 4.1 by

$$p_i = \frac{\lambda(r_0)}{\lambda(r_i)} \left(\frac{r_i}{r_0} \right)^2 \left\| \left(p_{dyn} \vec{e}_{flw} \right)_i \right\| \tag{17}$$

where r_i is the distance from the source origin (originally, the nucleus COM, see section 6.1).

Next, for each of the selected measurements, COMA_OP is called at the same time and angular position, but at a distance r_0 from the source origin. Let $p_{\mathrm{mod},i}$ denote these COMA_OP predictions.

For all selected measurements, the mean value of the ratio of measured to model dynamic pressure is calculated by

$$\mu = \frac{1}{n} \sum_{i=1}^{n} \frac{p_i}{p_{\mathrm{mod},i}} \tag{18}$$

Measurements can be used either to scale COMA_OP coefficients with a common factor preserving the underlying spatial distribution (update of gas production rate), or to modify the relative value of the coefficients or even alter the order of the spherical harmonics (update of spatial distribution). In the latter case, however, before increasing the order, it needs to be checked whether spherical harmonics as base functions are suitable to model the 3D morphology of the coma. Whatever the approach, extrapolation, i.e. use of the model to yield predictions at positions out of the region covered by the sample of measurements that were used to adjust the parameters of the model, shall be avoided.

To update COMA_OP without modifying the morphology of the coma, the spherical harmonics coefficients are multiplied with the factor μ. The residua $\Delta p_i = p_i - \mu p_{\mathrm{mod},i}$ can then be used to assess whether the resulting updated coma model results in an improvement of explaining past measured data. Before publishing the updated model for future use, it is checked that the planned future trajectory is inside the range where data were obtained in the past.

On the other hand, the spatial gas distribution is modeled correctly if the pressure error $\Delta p_i = p_i - \mu \ p_{\mathrm{mod},i}$ averaged on any subset of spherical coordinates $\{ \theta, \varphi \}$ contains zero within the error. Only if a reliable correlation of the pressure error versus spherical coordinates is observed repeatedly and over an extended period of time (e.g. several weeks), it is foreseen to update the spatial distribution defined by the spherical harmonic coefficients in COMA_OP.

To do so, a subset of data needs to be available that is suitable to perform the update. Before running this procedure, it needs to be validated that the temporal distribution is adequate for further use (see section 6.8). Once this is done, selected measurements $\left(p_{dyn} \vec{e}_{flw} \right)_i$ are scaled to the reference distance r_0 and reference heliocentric distance d_k by

$$p_i = \left(\frac{r_{h,i}}{d_k}\right)^{\alpha_k} \frac{\lambda(r_0)}{\lambda(r_i)} \left(\frac{r_i}{r_0}\right)^2 \left\|\left(p_{dyn}\vec{e}_{flw}\right)_i\right\| \tag{19}$$

where d_k and α_k are the parameters used in COMA_OP to model de dependency of comet outgassing on heliocentric distance (see section 4.1).

The coefficients of the spherical harmonics $\{a_0^0, a_l^0, a_l^m, b_l^m\}$ given in Eq. 5 are calculated as linear fit to the measured data $\{\theta_i, \varphi_i, p_i\}$ up to a certain order $l_{\max}$. The resulting fit can only be used for operations if the dynamic pressure is non-negative everywhere in the range where Rosetta operates.

6.8. Calibration of the temporal evolution

The change of the overall comet activity with heliocentric distance is modeled in COMA_OP by a power law versus heliocentric distance $(d_k/r_h)^{\alpha_k}$, where r_h is the heliocentric distance, and d_k and α_k are piece-wise defined parameters (see section 4.1).

For each range of heliocentric distances k, it is validated that the value of the slope α_k is supported by measurements by fitting $\Delta\alpha_k$ in the equation

$$p_i = \mu p_{\text{mod},i} \left(\frac{d_k}{r_{h,i}}\right)^{\Delta\alpha_k} \tag{20}$$

where p_i and $p_{\text{mod},i}$ are measured and modeled dynamic pressures, as defined in the previous section (p_i values are calculated with Eq. 17).

Measurements are selected for the fit based on the underlying observable (torque, ROSINA or MIRO), and appropriate intervals of times and cometocentric distances. It is important to only use measurements made over the same point on the nucleus at the same rotational phase relative to the Sun. This is necessary in order to avoid that a mismodeling in the spatial distribution is falsely attributed to a change in overall activity.

Ideally, several such fits should be made over different points and rotation angles of the nucleus. Only if all fits give consistent non-zero results for $\Delta\alpha_k$ for a sufficiently long arc of data (at least several weeks) an update of the temporal evolution is done by adding $\Delta\alpha_k$ to the value α_k in COMA_OP. After an update of α_k, the procedure in section 6.7 needs to be run.

6.9. Comparison of gas and dust distributions

Optical images of the coma are expected to be dominated by light scattered by dust, whereas the dynamic pressure is expected to be dominated by gas molecules. Therefore an estimate of the dynamic pressure from optical images is a very indirect method and requires establishing an empirical scaling law first. The aim of the procedure described in this section is to help establishing such a scaling law.

Inputs to the method are a subset of the binned camera images obtained with the procedure described in section 3.2.2. Estimates of $J/I_{sun}^{(filter)}$ and the $Af\rho$-value are used to fit the spatial dust distribution on a reference sphere under certain assumptions. In particular, it is assumed that the dust coma is optically thin in visual wavelength. Moreover, in the part of the coma covered by the selected images, particles can be well described by a single effective dust class (this means that e.g. fragmentation of particles is of minor importance) with constant velocity and the same optical properties everywhere.

The obtained fit is then compared to the spatial distribution of gas to derive guidelines that allow to extract information of coma gas from images of the dust taken with the onboard cameras.

6.10. Further model adjustments

If the coma turns out to be very predictable, adjustments of the models beyond those mentioned in sections 6.2 to 2.9 may be possible.

Regarding COMA_OP parameters, it might be possible to offset the origin of the single species source from the nucleus COM to improve predictions, or even increase the number of sources with new sources attached to the nucleus or with different sources for each gas species. In either case, flow direction $\vec{e}_{flw}$ would stop being parallel to the vector of position relative the nucleus center. It may also be possible to define the spherical harmonics coefficients as a function of time via Fourier series, to incorporate cyclical variations of activity tied to the nucleus rotation. Finally, a set of base functions other than spherical harmonics might be defined if spherical harmonics are no suitable to represent the morphology of the coma.

Regarding COMA_DRAG, it will be considered to adjust the accommodation coefficient of each SC surface to observed drag torque if the hypothesis of perfectly inelastic collisions proves unrealistic.

The specific procedures to implement these adjustments are out of the scope of this document.

7. References

[1] Keller, H.U. el al. "OSIRIS – The scientific camera system onboard Rosetta." Space Science Reviews, Vol. 128, Issue 1-4, pp. 433-506, 2007.

[2] Gulkis S. et al. "MIRO: Microwave Instrument for Rosetta Orbiter." Space Science Reviews, Vol. 128, pp. 561-597, 2006.

[3] AIRBUS Defence & Space (formerly EADS Astrium), *Rosetta Users Manual*, Issue 5, Drawing Rosetta Flight Configuration 2480-100-002A00C in Appendix 9 - Spacecraft Configuration Drawings, 2003. Modified with permission from ROSETTA Project Manager at AIRBUS.

[4] Bielsa, C., Müller, M. and Huguet, G. "Prediction of the coma drag force on Rosetta." Proceedings 23th International Symposium on Space Flight Dynamics - 23th ISSFD. JPL, Pasadena, California, USA, 2012.